Al doped graphene: A promising material for hydrogen storage at room temperature

Z. M. Ao,[1,2] Q. Jiang,[2,a)] R. Q. Zhang,[2] T. T. Tan,[1] and S. Li[1,a)]
[1]*School of Materials Science and Engineering, The University of New South Wales, New South Wales 2052, Australia*
[2]*Department of Materials Science and Engineering and Key Laboratory of Automobile Materials, Ministry of Education, Jilin University, Changchun 130025, China*

(Received 16 January 2009; accepted 18 February 2009; published online 3 April 2009)

A promising material for hydrogen storage at room temperature–Al doped graphene is proposed theoretically by using density functional theory calculation. Hydrogen storage capacity of 5.13 wt % is predicted at $T=300$ K and $P=0.1$ GPa with an adsorption energy $E_b=-0.260$ eV/H_2. This is close to the target specified by U.S. Department of Energy with a storage capacity of 6 wt % and a binding energy of -0.2 to -0.4 eV/H_2 at ambient temperature and modest pressure for commercial applications. It is believed that the doped Al alters the electronic structures of both C and H_2. The bands of H_2 overlapping with those of Al and C simultaneously are the underlying mechanism of hydrogen storage capacity enhancement. © *2009 American Institute of Physics*. [DOI: 10.1063/1.3103327]

I. INTRODUCTION

In recent years, hydrogen-based fuel systems have been considered to be a highly important topic of research for future energy schemes as hydrogen is a more efficient fuel in comparison to the existing carbonaceous fossil fuels.[1,2] Despite many recent technological developments in the hydrogen-based fuel systems, it is still an enormous challenge to have safe and efficient reversible hydrogen storage systems at ambient conditions.[2] One possible way for hydrogen storage is an efficient and controllable adsorption/desorption system. Carbon based materials appear promising for such a purpose. Although several mechanisms of hydrogen storage through both physisorption and chemisorption have been proposed,[3–7] most of these efforts are far to reach the target of 6 wt % and binding strength of -0.2 to -0.4 eV/H_2 at ambient temperature and modest pressure for commercial applications specified by U.S. Department of Energy (DOE).

With density functional theory (DFT) simulations, it was predicted that a single ethylene molecule can form a stable complex with two transition metals, thus adsorbing ten H_2 molecules and lead to a high storage capacity of ~14 wt %.[8] In addition, the highest H_2 storage capacity of 13 wt % in a fullerene cage with 12 Li atoms capped onto the pentagonal faces was calculated.[9] This system has average adsorption energy $E_b=-0.075$ eV/H_2. However, all the DFT results are in the ideal condition at the temperature of $T=0$ K; their performances at the DOE specified operation conditions are unclear.

Since carbon nanostructures have high surface areas and thermal stability along with unique mechanical properties, improvement of their adsorption capacity by suitable modification would be of immense interest.[3–9] Thus, hydrogen storage using carbon nanostructures is still an important issue and deserves more attention. In this work, the potential of graphene as hydrogen storage materials through doping is investigated. The advantages of graphene are as follows: (1) a large surface for hydrogen adsorption, (2) economical and scalable production,[10] and (3) the strongest material ever measured.[11]

AlH_3 and related aluminum hydrides as hydrogen storage materials have recently become the focus of renewed interest[12,13] as their potentially large hydrogen capacity of ~10 wt %. These materials are thermodynamically unstable in ambient, but it is kinetically stable without much lost of hydrogen for years. Despite these excellent properties, extremely high pressure (exceeding 2.5 GPa) is required for hydrogen adsorption. While these hydrides possess a small negative enthalpy of formation,[13] for practical applications, the large hydrogen desorption energy proves impractical. The origin of this energy barrier lies in the rather strong mixed ionic and covalent bonds[13] formed between Al and H. Thus it is essential to significantly reduce the desorption energy.

There appears another way for Al atoms to store hydrogen, i.e., to further decrease the interaction between Al and H. In this way, the weak chemisorption can be changed into strong physisorption. For hydrogen storage through physisorption, strong interaction between the H_2 molecule and the surfaces along with a large surface area for adsorption is required. The unique characteristics of graphene and Al for hydrogen storage lead to an investigation of the properties of Al doped graphene as a possible hydrogen storage candidate. It would be intriguing to understand the interaction between graphene, Al, and H. In this work, the adsorption behavior of H_2 in Al doped graphene was studied by DFT calculation. In addition, we processed the *ab initio* molecular dynamics (MD) calculation to investigate the effects of temperature and pressure on the corresponding adsorption and desorption behaviors of this system.

a)Authors to whom correspondence should be addressed. Electronic addresses: jiangq@jlu.edu.cn and sean.li@unsw.edu.au.

II. CALCULATION METHODOLOGY

All DFT calculations are performed in DMOL3 code.[14] Previous studies[15,16] have shown that the local density approximation (LDA) prediction of the physisorption energies of H_2 on the surface of graphite and carbon nanotubes is in good agreement with experiments. The reliability of LDA can be ascribed to the following facts.[15] (1) When the electron densities of H_2 and graphene overlap weakly, the nonlinearity of the exchange-correlation energy density functional produces an attractive interaction even in the absence of electron density redistribution. (2) The overestimated binding energy by LDA (Refs. 17 and 18) may compensate for the insufficient account of van der Waals interactions.[15] In contrast, DFT calculation using a uniform generalized gradient approximation (GGA) produced a purely repulsive interaction. Using a GGA-PW91 functional, a repulsive interaction between H_2 and a graphene layer and also between H_2 and a (6,6) carbon nanotube was obtained.[19] This contradicts the experimental findings.[20] It was noted that LDA calculations well reproduce the empirical interaction potentials between graphitic layers and also in the other graphitic systems for distances near the equilibrium separation although the LDA is not able to reproduce the long-range dispersion interaction.[21] Therefore, LDA is selected in this work. To ensure that the calculated results are comparable, identical conditions are employed for the isolated H_2 molecules and the graphene and also the adsorbed graphene system. The k-point is set to $6\times6\times2$ for all slabs, which brings out the convergence tolerance of energy of 1.0×10^{-5} hartree (1 hartree=27.2114 eV) and that of maximum force is 0.002 hartree/Å.

In the simulation, three-dimensional periodic boundary condition is taken and H–H bond length is set to $l_{H-H}=0.74$ Å, which is consistent with the experimental results.[22] The graphene used in our simulation consists of a single layer of 3×3 supercell with a vacuum width of 12 Å to minimize the interlayer interaction. Increasing the vacuum width will greatly increase the computation expense although it has only negligible consequence on the results obtained. All atoms are allowed to relax in all energy calculations. The adsorption energy E_b between the H_2 gas molecule and graphene is defined as

$$E_b = E_{H_2+\text{graphene}} - (E_{\text{graphene}} + E_{H_2}), \quad (1)$$

where the subscripts H_2+graphene, graphene, and H_2 denote the adsorbed system, isolated graphene, and H_2 molecules, respectively.

For the Al doped graphene, the concentration of Al is 12.5 at. % with the additional constraint that there is only one Al atom per graphene hexagonal ring (Fig. 1) to avoid Al atoms clustering on graphene.[23] For H_2 adsorption on the Al doped graphene, there are four top sites of T1, T2, T3 and T4, three bridge sites of B1, B2, and B3, and two center sites of C1 and C2, as shown in Fig. 1. (In this figure, a larger simulation cell is given in order to better display the different adsorption sites on the Al doped graphene. Figure 2 reflects the actual simulation cell size.) At each adsorption site, there are two highly symmetrical adsorption configurations, namely, H_2 molecule resides parallel or perpendicular to the graphene surface. Therefore, a total of 18 adsorption configurations for H_2 on the Al doped graphene is present.

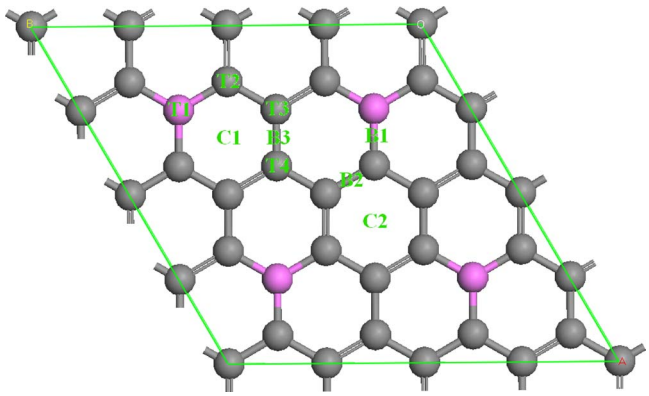

FIG. 1. (Color online) Nine different adsorption sites on the Al doped graphene. The gray and pink balls are, respectively, C and Al atoms.

Due to the periodicity of H_2 adsorbed in intrinsic graphene or Al-doped-graphene systems, we have selected the unit cell with the following conditions: eight C atoms and one H_2, or seven C atoms, one Al atom, and one H_2 (see Fig. 2). If we place a H_2 at any location of the cell, the distance from this H_2 to other H_2 molecules in the nearest cells is 4.920 Å. This large separation, compared to the bond length of H_2 (0.740 Å), would ensure that there is no interaction between H_2 molecules in the different cells.[24]

To calculate the H_2 adsorption capability of Al doped graphene at room temperature and modest pressure, we performed *ab initio* MD calculation with Cambridge sequential total energy package (CASTEP) code based on the structure obtained by DFT above, which utilizes plane-wave pseudopotential to perform the first principles quantum mechanics calculations.[25] LDA with the Ceperley–Alder–Perdew–Zunger function[26,27] was employed as exchange-correlation

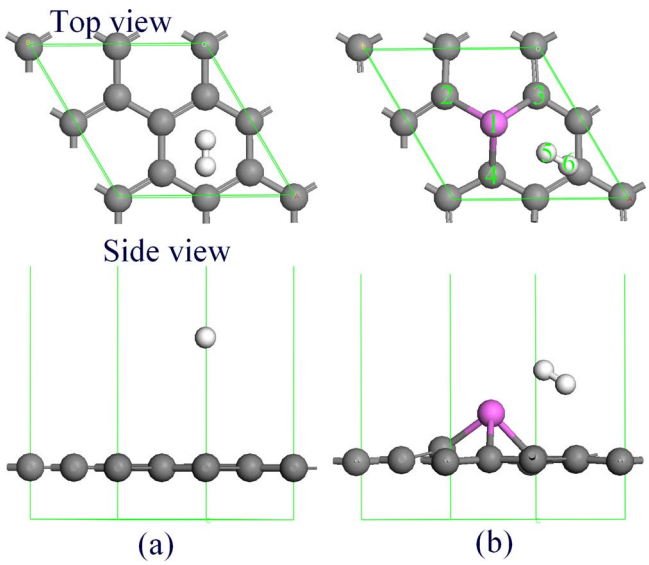

FIG. 2. (Color online) The favorite adsorption configurations with one H_2 molecule adsorbed in (a) intrinsic graphene and in (b) Al doped graphene. The gray and pink balls have the same meaning in Fig. 1, and the white balls are H atoms.

TABLE I. Summary of results for H_2 adsorption on intrinsic graphene and Al doped graphene on different adsorption sites. For H_2 adsorption on intrinsic graphene, there are six different adsorption sites as listed in the table. For H_2 adsorption on Al doped graphene, there are 18 different adsorption configurations, as shown in Fig. 1.

		Intrinsic graphene		Al doped graphene		
Initial binding configuration		E_b (eV)	d (Å)[a]	E_b (eV)	l (Å)[b]	d (Å)[a]
H_2//graphene	T1	−0.136	2.845	−0.209	2.762	
	T2			−0.34	2.526	2.682
	T3			−0.407	2.588	2.486
	T4			−0.361	2.942	2.537
	B1	−0.139	2.817	−0.21	2.757	
	B2			−0.411	2.527	2.575
	B3			−0.411	2.506	2.563
	C1	−0.159	2.635	−0.427	2.083	2.073
	C2			−0.188		2.657
$H_2 \perp$ graphene	T1	−0.141	2.615	−0.153	2.622	
	T2			−0.284	2.427	2.749
	T3			−0.406	2.367	2.524
	T4			−0.33	2.976	2.179
	B1	−0.142	2.620	−0.206	2.271	3.732
	B2			−0.412	2.468	2.595
	B3			−0.426	3.196	2.074
	C1	−0.148	2.425	−0.426	2.092	2.104
	C2			−0.24	3.117	2.468

[a]Distance between H_2 molecule and graphene or Al-doped-graphene layer.
[b]Distance between Al and H_2.

functions, cutoff energy E_c=280 eV, and k-points is 6×6×2. In principle, E_c increases until the calculated total energy converges within the required tolerance. $dE_{tot}/d \ln E_c$ is the parameter used to evaluate the accuracy of the calculation, where E_{tot} is the total energy of the system. The software can calculate $dE_{tot}/d \ln E_c$ value automatically. In general, $dE_{tot}/d \ln E_c$=0.1 eV/atom is sufficient for the most calculations. The values of k-points are increased until the calculated energy converges within the required tolerance, where the k-points sample the irreducible wedge of the Brillouin zone. In this work, the k-points of 6×6×2 for all slabs have the energy convergence tolerance of 1.0×10^{-6} eV/atom. Such energy tolerance is small enough to ensure establishment of the actual equilibrium structure.

Each MD simulation was performed in *NPT* statistical ensemble, i.e., constant numbers of atoms N, pressure P, and T, with T=300 K and P=0.0001–1 GPa. A time step of 1 fs was selected and simulation time t at a particular T was 2.5 ps where the total energy fluctuation was in the range of 0.01%. The same t was selected for H_2S dissociation on the Fe(110) surface.[28] A Verlet algorithm[29] was used to integrate the equations of motion, with T controlled by algorithm of Nose,[30] and P was controlled according to the Parrinello–Raham algorithm.[31] A key parameter in the integration algorithms is the integration time step. A common rule of thumb used to set the time step is that the highest frequency vibration should be sampled between 10 and 20 times in 1 cycle. In this system, the frequency is in the order of 10^{13} Hz;[32] the time step is thus set as 1 fs within a reasonable range.

III. RESULTS AND DISCUSSION

After geometry relaxation, E_b values and the corresponding structure parameters of the six adsorption configurations for H_2 adsorbed in the intrinsic graphene are listed in Table I. It was found that the most favorable configuration is H_2 adsorbed on the center site of the carbon ring with E_b=−0.159 eV as shown in Fig. 2(a) and the distance between H_2 and the graphene is d=2.635 Å. The results are consistent with other reported results of E_b=−0.133 eV and $d \approx 2.8$ Å.[16] The small magnitude of E_b shows that the system is in the weak physisorption region. It indicates that the intrinsic graphene is not suitable for hydrogen storage under the postulated operating conditions.

For the adsorption of H_2 in the Al doped graphene, the corresponding results are also listed in Table I. As can be seen from Table I, the most favorable position with E_b =−0.427 eV for the H_2 molecule is shown in Fig. 2(b). The distance between H_2 and the doped Al is l=2.083 Å while that between H_2 and carbon layer is d=2.073 Å. As seen from Table I, the interaction reaches the strongest when both l and d are minimized. The adsorption of H_2 in the Al doped graphene is larger than that in other systems, such as E_b=−0.41 eV/H_2 in the Ti–C_2H_4-graphene system[8] and E_b=−0.08 eV/H_2 in 12-Li-doped fullerene.[9] However, this still belongs to the physisorption system as the long distance between the doped graphene and the adsorbed H_2. Therefore, this strong physisorption interaction would be ideal for hydrogen storage, which can adsorb more H_2 molecules.

To understand the enhancement effect of the doped Al on

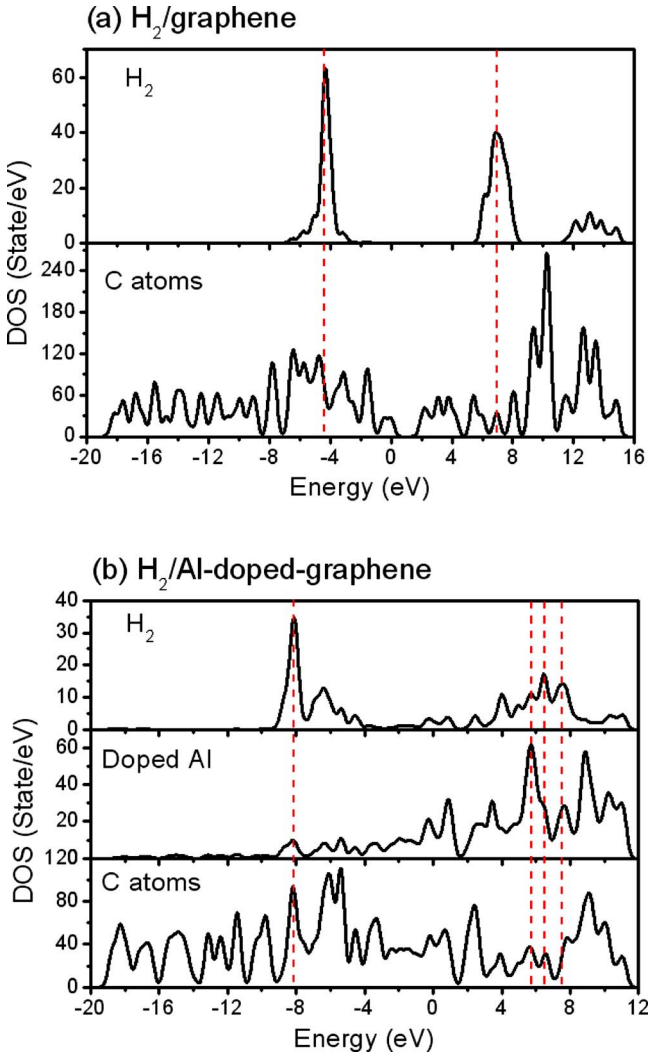

FIG. 3. (Color online) The PDOS of adsorbed H_2, doped Al, and graphene in both the H_2/graphene and H_2/Al-doped-graphene systems, as shown in panels (a) and (b), respectively. Fermi level is set to 0.

the H_2 adsorption, the projected electronic density of states (PDOS) of the adsorbed H_2, the doped Al, and the C atoms in both H_2/graphene and H_2/Al-doped-graphene systems are plotted and shown in Fig. 3. Figure 3(a) shows the PDOS of H_2/graphene system. The main peaks of H_2 are located at −4.37 and 6.92 eV. However, the main peaks of intrinsic graphene are located between 9 and 13 eV. Therefore, the interaction between H_2 molecule and the intrinsic graphene is very weak because of nonoverlapping of electrons in these substances, where E_b is small. On the other hand, for the H_2/Al-doped-graphene system shown in Fig. 3(b), the main peaks of H_2 are located at −8.15, 5.74, 6.52, and 7.51 eV, respectively. The bands of H_2 interact with both the doped Al and the C atoms simultaneously at the positions indicated by the dashed lines, showing a strong interaction between H_2 and the Al doped graphene where E_b is the largest. In addition, the doped Al changes the electronic structures of both H_2 and the graphene, and both their PDOSs shift toward the lower energy. This suggests that the H_2/Al-doped-graphene configuration is a much more stable system.

Table II shows the charge distribution in both the H_2/graphene and H_2/Al-doped-graphene systems using Mulliken analysis. Before and after H_2 adsorption, the charge variation for the former is little while it is significant for the latter. In addition, H6 has much more positive charge than H5. Thus, the interaction between H_2 and the Al doped graphene is mainly achieved through H6. The interaction between the band at the location of the highest peak of PDOS plot of H_2 and that of C atoms implies a strong interaction between the H_2 and C atoms, as shown in Fig. 3(b).

TABLE II. Charges of atoms in H_2 adsorbed in graphene system as well as charge transfer Q between graphene and H_2 molecule obtained by Mulliken analysis. The unit of the atom charge is one electron charge e, which is elided here for clarity.

Atom	Intrinsic graphene	Al doped graphene
Al1 (C1)	0.001	0.292
C2	−0.002	−0.228
C3	0	−0.193
C4	0	−0.193
H5	−0.001	−0.001
H6	−0.001	0.021
Q	−0.002	0.019

The illustrations of electron density distribution for the H_2/graphene and H_2/Al-doped-graphene systems are shown in Fig. 4. In the system of H_2/graphene [Fig. 4(a)], no electron exists in the region between H_2 and C layer while some electrons appear in the region among H_2, Al atom, and C layer in the system of H_2/Al-doped-graphene [Fig. 4(b)]. This supports the notion that the H_2/Al-doped graphene possesses a much stronger H_2 adsorption ability.

After understanding the mechanism of the enhancement for H_2 adsorption in the Al doped graphene, it is important to determine how much H_2 molecules can be adsorbed on the 3×3 layer surface. We constructed an adsorption configuration with three H_2 molecules adsorbed in the three favorable C1 adsorption positions on the top side of the doped system. After geometry relaxation, the atomic structure is shown in Fig. 5(a). It has E_b=−0.303 eV/H_2, which satisfies the requirement of E_b=−0.20 to −0.40 eV/H_2 at room temperature[3–6] set by DOE although the value of 5.1 wt % of H_2 adsorbed is slightly below the DOE's 6 wt % target.

In order to understand the effect of the adsorbed H_2 molecule number on the E_b, the configuration with six H_2 molecules adsorbed in the Al doped graphene in the favorable C1 adsorption positions on both sides was calculated. It is found that E_b=−0.164 eV/H_2, which is much smaller than

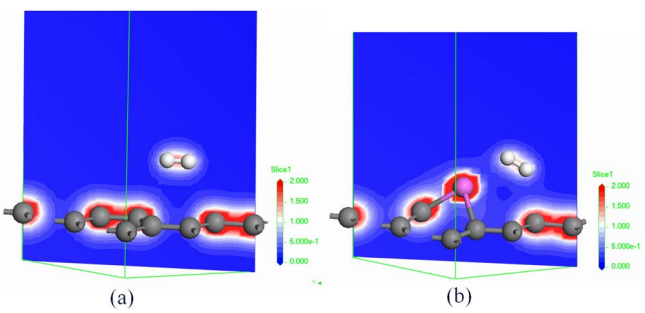

FIG. 4. (Color online) Electron density distributions in the H_2/graphene [panel (a)] and H_2/Al-doped-graphene [panel (b)] systems.

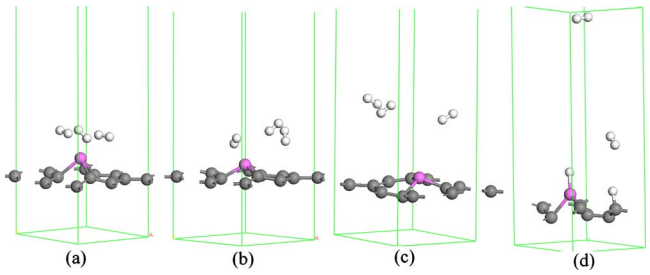

FIG. 5. (Color online) Atomic configurations of three H_2/Al-doped-graphene system at different temperatures and pressures. (a) In the ideal condition with $T=0$ K, (b) in the condition with $T=300$ K and $P=0.1$ GPa, (c) in the condition with $T=300$ K and $P=0.0001$ GPa, and (d) in the condition with $T=300$ K and $P=1$ GPa.

the E_b for the above case where the Al doped graphene adsorbed three H_2 on one side of graphene. In addition, the adsorption with eight H_2 molecules in the Al doped graphene was also calculated, and it is found that two H_2 molecules were released. In other words, the interaction between H_2 molecules would weaken the adsorption and the saturated number of H_2 molecules adsorption is 6. Note that E_b for the cases of three H_2 and six H_2 are, respectively, -0.303 and -0.164 eV/H_2, which is about twice for the case of three H_2 compared with the case of six H_2. This is because H_2 molecules were very weakly adsorbed below the graphene layer where the doped Al atom locates above the graphene layer.

It is well known that increasing pressure (P) and decreasing temperature (T) enhance the capacity of hydrogen storage. Thus, most studied systems are either under high P or at very low T,[20] which may not be viable for mobile applications. For example, it has been reported that purified single wall carbon nanotubes (SWNTs) has a storage capacity of 8 wt % at 80 K with a hydrogen pressure of 13 MPa (Ref. 33) but has only a much lower hydrogen storage capacity of 2.3 wt % at 77 K.[34] The hydrogen storage capacities in other carbon related materials, such as activated carbon (AC), single walled carbon nanohorn, SWNTs, and graphite nanofibers, were also reported.[35] Although the AC had a capacity of 5.7 wt % at 77 K with $P=3$ MPa, its capacity is $<1\%$ at 300 K.[35] Recent experimental results demonstrated that the intrinsic graphene has hydrogen storage capacity of 1.7 wt % under 1 atm at 77 K and of 3 wt % under 100 atm at 298 K.[36] Thus, to meet the DOE target, it is necessary to study the adsorption and desorption behaviors of H_2 in the Al doped graphene at $T=300$ K with different P. Therefore, the adsorption behaviors of three H_2/Al-doped-graphene and six H_2/Al-doped-graphene systems were calculated under 0.0001, 0.01, 0.1, and 1 GPa using *ab initio* MD simulation. For both the three H_2/Al-doped-graphene and six H_2/Al-doped-graphene systems, we found that all H_2 molecules were released at 0.0001 GPa [Fig. 5(c)]. However, there was only one H_2 molecule adsorbed in both the systems at 0.01 GPa, while the structure of the doped graphene was completely destroyed with H and Al forming covalent bond at 1 GPa [Fig. 5(d)]. When $P=0.1$ GPa, there are three H_2 left on the top side of the two Al doped systems [Fig. 5(b)]. Therefore, the Al doped graphene for hydrogen storage capacity at room temperature and 0.1 GPa is 5.13 wt % with $E_b=-0.260$ eV/H_2, satisfying the requirements of actual application. In addition, all the adsorbed H_2 molecules can be released when $P=0.0001$ GPa.

IV. CONCLUSION

In conclusion, the adsorption behaviors of H_2 in the intrinsic and Al doped graphene were studied using DFT. It is found that the physisorption of H_2 is greatly enhanced by doping Al into graphene. The doped Al varies the electronic structures of both C and H_2, causing the bands of H_2 overlapping with those of Al and C simultaneously. It induces an intensive interaction between H_2 and the Al doped graphene. This was also demonstrated by the electron density distribution. In order to understand the temperature and pressure effects on the H_2 adsorption behavior for actual application, *ab initio* MD calculations for the H_2/Al-doped-graphene system were processed. It is found that the system has 5.13 wt % hydrogen storage ability at $T=300$ K with $P=0.1$ GPa. Therefore, the Al doped graphene would be a promising hydrogen storage material owing to the strong interaction between H_2 and the Al doped graphene.

ACKNOWLEDGMENTS

This work was financially supported by the National Key Basic Research and Development Program (Grant No. 2004CB619301), "985 Project" of Jilin University, and Australia Research Council Discovery Program Contract No. DP0665539.

[1] R. Coontz and B. Hanson, Science **305**, 957 (2004).
[2] L. Schlapbach and A. Züttel, Nature (London) **414**, 353 (2001).
[3] E. Klontzas, A. Mavrandonakis, E. Tylianakis, and G. E. Froudakis, Nano Lett. **8**, 1572 (2008).
[4] G. Mpourmpakis, E. Tylianakis, and G. E. Froudakis, Nano Lett. **7**, 1893 (2007).
[5] K. R. S. Chandrakumar and S. Ghosh, Nano Lett. **8**, 13 (2008).
[6] W. Q. Deng, X. Xu, and W. A. Goddard, Phys. Rev. Lett. **92**, 166103 (2004).
[7] A. Nikitin, X. Li, Z. Zhang, H. Ogasawara, H. Dai, and A. Nilsson, Nano Lett. **8**, 162 (2008).
[8] E. Durgun, S. Ciraci, W. Zhou, and T. Yildirim, Phys. Rev. Lett. **97**, 226102 (2006).
[9] Q. Sun, P. Jena, Q. Wang, and M. Marquez, J. Am. Chem. Soc. **128**, 9741 (2006).
[10] D. Li, M. B. Müller, S. Gilje, R. B. Kaner, and G. G. Wallace, Nat. Nanotechnol. **3**, 101 (2008).
[11] C. Lee, X. Wei, J. W. Kysar, and J. Hone, Science **321**, 385 (2008).
[12] X. Li, A. Grubisic, S. T. Stokes, J. Cordes, G. F. Ganteför, K. H. Bowen, B. Kiran, M. Willis, P. Burgert, and H. Schnöckel, Science **315**, 356 (2007).
[13] J. Graetz, S. Chaudhuri, Y. Lee, T. Vogt, J. T. Muckerman, and J. J. Reilly, Phys. Rev. B **74**, 214114 (2006).
[14] B. Delley, J. Chem. Phys. **92**, 508 (1990).
[15] I. Cabria, M. J. López, and J. A. Alonso, J. Chem. Phys. **128**, 144704 (2008).
[16] Y. Okamoto and Y. Miyamoto, J. Phys. Chem. B **105**, 3470 (2001).
[17] A. Lugo-Solis and I. Vasiliev, Phys. Rev. B **76**, 235431 (2007).
[18] O. Leenaerts, B. Partoens, and F. M. Peeters, Phys. Rev. B **77**, 125416 (2008).
[19] K. Tada, S. Furuya, and K. Watanabe, Phys. Rev. B **63**, 155405 (2001).
[20] U. Sahaym and M. G. Norton, J. Mater. Sci. **43**, 5395 (2008).
[21] L. A. Girifalco and M. Hodak, Phys. Rev. B **65**, 125404 (2002).
[22] D. R. Lide, *CRC Handbook of Chemistry and Physics*, 81st ed. (CRC, Boca Raton, FL, 2000).

[23]P. O. Krasnov, F. Ding, A. K. Singh, and B. I. Yakobson, J. Phys. Chem. C **111**, 17977 (2007).
[24]J. S. Arellano, L. M. Molina, A. Rubio, and J. A. Alonso, J. Chem. Phys. **112**, 8114 (2000).
[25]M. D. Segall, P. L. D. Lindan, M. J. Probert, C. J. Pickard, P. J. Hasnip, S. J. Clark, and M. C. Payne, J. Phys.: Condens. Matter **14**, 2717 (2002).
[26]D. M. Ceperley and B. J. Alder, Phys. Rev. Lett. **45**, 566 (1980).
[27]J. P. Perdew and A. Zunger, Phys. Rev. B **23**, 5048 (1981).
[28]M. J. S. Spencer and I. Yarovsky, J. Phys. Chem. C **111**, 16372 (2007).
[29]L. Verlet, Phys. Rev. **159**, 98 (1967).
[30]S. Nose, Prog. Theor. Phys. Suppl. **103**, 1 (1991).
[31]M. Parrinello and A. Rahaman, J. Appl. Phys. **52**, 7182 (1981).
[32]A. Gross and M. Scheffler, Prog. Surf. Sci. **53**, 187 (1996).
[33]Y. Ye, C. C. Ahn, C. Witham, B. Fultz, J. Liu, A. G. Rinzler, D. Colbert, K. A. Smith, and R. E. Smalley, Appl. Phys. Lett. **74**, 2307 (1999).
[34]B. Panella, M. Hirscher, and S. Roth, Carbon **43**, 2209 (2005).
[35]W. C. Xu, K. Takahashi, Y. Matsuo, Y. Hattori, M. Kumagai, S. Ishiyama, K. Kaneko, and S. Iijima, Int. J. Hydrogen Energy **32**, 2504 (2007).
[36]A. Ghosh, K. S. Subrahmanyam, K. S. Krishna, S. Datta, A. Govindaraj, S. K. Pati, and C. N. R. Rao, J. Phys. Chem. C **112**, 15704 (2008).